

## Turbulence in microwave electronics: Theoretical approaches and experimental results

*D. I. Trubetskov<sup>1,2</sup>, Yu. A. Kalinin<sup>1</sup>, A. V. Starodubov<sup>1</sup>, A. S. Fokin<sup>1</sup>*

<sup>1</sup>National Research Saratov State University  
Astrahanskaya, 83, 410012 Saratov, Russia

<sup>2</sup>National Research Nuclear University «MEPhI»  
Kashirskoe shosse, 31, 115409 Moscow, Russia  
E-mail: [dtrubetskov@yahoo.com](mailto:dtrubetskov@yahoo.com); [noios@sgu.ru](mailto:noios@sgu.ru);

[StarodubovAV@gmail.com](mailto:StarodubovAV@gmail.com); [alexander1989fokin@mail.ru](mailto:alexander1989fokin@mail.ru)

A review of the current state of different theoretical approaches to the description of turbulence in electron beams and electronic devices at microwave frequencies is shown. A three types of turbulent (nonlaminar) electron beams were considered. The first type of turbulent electron beam is caused by the intersection of electronic trajectories (e.g., due to thermal velocity) and it is common to the flow of electrons at all. The turbulence of the second type is due to the instability of the electron beams, because of which a small perturbations grow for an exponentially (such instabilities include diocotron and slipping-instability). The third type – vortex turbulence, the cause of which is filamentarization of electron flow. Formed charged filaments interact among themselves, that leads to the formation of vortex structures; the presence of this structures increases the number of collective degrees of freedom and may lead to turbulence. The results of an experimental study of turbulent flows and electronic generators with their use in standalone mode and when an external signal were shown. Various types of broadband microwave oscillators oscillations were investigated. We discuss the phenomenological model of turbulent the electron beam, which is a chain of superradiant clots containing electron-oscillators, chain of «vortices» («vortices» are describes by the modified equations of van der Pol).

*Keywords:* electron flow, turbulence, instability, vortex, generator, broadband microwave generation

DOI: 10.18500/0869-6632-2016-24-5-4-36

*Paper reference:* Trubetskov D.I., Kalinin Yu.A., Starodubov A.V., Fokin A.S. Turbulence in microwave electronics: Theoretical approaches and experimental results. *Izvestiya VUZ. Applied Nonlinear Dynamics*, 2016, vol. 24, iss. 5. P. 4–36.

*The work is supported by the RFBR grants 16-02-00238, 14-02-00329, and by Ministry of Education and Science of the Russian Federation.*

## Introduction

Turbulence research has a long history dating back to Leonardo da Vinci. Among his notes there is an amazing fragment: he introduces 64 terms from hydrodynamics, accompanying them with drawings. It's a peculiar scientific-artistic encyclopedia of nonlinear waves with an accent on turbulence, which doesn't correspond to its time, but gets ahead of time; it amazed and continues to amaze the researches of Leonardo's creation in all the times. Subsequently turbulence at different levels has been studied in liquids and gases, in plasma, in environmental and biochemical media. There are significantly less studies of turbulence in microwave electronics, to which this review is devoted to. There are many different definitions of turbulence. Further we follow such a definition: turbulence is a state of the medium, when which the movements (turbulent pulsations) of different scale are excited, moreover there is a transfer of energy between them. Under "scale" we understand the order of magnitude of those distances during which the speed of movement changes significantly. It's important to emphasize that turbulent pulses are of inherently random character.

In connection with the creation of vacuum generators of noise and chaotic microwave oscillations there appeared a problem in understanding the occurrence of such fluctuations and their connection with the turbulence of electron beams. There are still few works in which the turbulence of electron beams is discussed. These works can be divided in three groups. The *first group* should include the results of the works on non-laminar electron beams, in which the turbulence is caused by crossing of electron trajectories, for example, because of thermal velocities. In the works of the *second group* the appearance of turbulence is explained by non-stability of small perturbations in electron beams, which increase exponentially and when large amplitudes are reached, they lead to turbulence. The third group included the works discussing vortex turbulence or, more common, a turbulence associated with the formation and interaction of coherent structures in electron beam. Further we consider different basic works belonging to these three groups.

### 1. Some theoretical models of turbulence in electron beams and their analysis

The results of the first group of works are set out in the papers [1, 2]. Formally the initial model of this group shows that there is no closed system of hydrodynamical equations describing electron beams. Thus there arises a circuit problem like the similar one in classical theory of turbulent liquids. This allows to study turbulent electron beams in the frames of hydrodynamical theory, as very slightly differing from laminar ones. In the work [1] one can find the analysis of stationary plain beam in crossed static electric and magnetic fields. The structure of pressure tensor is put in phenomenologically. Standard for a similar approach in the theory of fluid turbulence analysis showed that the presence of turbulence in electron beam requires increasing of magnetic field, necessary for forming beams close to Brillouin laminar beams, for which plasma frequency is exactly equal to cyclotron one. In the paper [2] the similar non-linear model is called "quasi-Brillouin beam".

As indicated in the introduction, the second group of works includes articles in which the occurrence of turbulence is associated with the instability of electron flows, when infinitely small perturbations increase exponentially in space or/and in time, while nonlinearity leads to turbulence. The other model is supposed to be stable to small perturbations, but an electron beam is able to get into a turbulent state with suitable disturbances of finite value. As a rule, the first model is analysed, although, apparently, turbulence can occur in both cases. Most often in connection with the analysis of turbulence, diocotron and slipping instabilities are investigated (see for example [3–12]).

Diocotron instability occurs in a drifting tubular electron beam, moving in longitudinal magnetic field and inhomogeneous electric field of the beam space charge [4, 14]. It is close to instability of thin charged layers in crossed electrostatic and magnetostatic fields, for which a simple physical explanation

for instability is possible (see, for example [13]). Really, if solving a problem of tubular beam, we go to a coordinate system, moving along a magnetic field with a velocity equal to the static velocity of electron beam, then the movement of electrons will be similar to the situation in crossed fields – perpendicular to electric and magnetic fields. In thin band layer in crossed fields the local increasing of space charge density leads to bending of the layer, it becomes unstable, and the initial perturbation increases. We remind (according to [13, ch. 5]) a qualitative picture of the occurrence of instabilities in the electron beam in crossed fields, Let's consider a beam with finite depth  $L$  in crossed beams, which is moving between two plains, and the electron paths are straightforward. In the longitudinal direction  $x$ , the flow is infinite and homogeneous. This allows, in the two-dimensional approximation, to assume that there is only a transverse  $y$ -component of the static field of the space charge and

$$\frac{\partial E_0}{\partial y} = \frac{\rho_0(y)}{\varepsilon_0},$$

where  $\rho_0(y)$  is the space charge density in the beam. It's not equal to zero in the frames of beam depth  $\Delta$ , and is some arbitrary function of coordinate  $y$ . Let's note that  $E_0$  is the sum of space charge field  $\tilde{E}_0$  and external static field  $\bar{E}_0$ ;  $y_0 - \Delta/2 \leq y \leq y_0 + \Delta/2$ ;  $\varepsilon_0$  is the dielectric constant of vacuum. The straightness of the trajectories requires the electron velocity to be determined by the formula  $v_0 = E_0/B$  ( $B$  is the static magnetic induction) and consequently

$$\frac{\partial v_0}{\partial y} = \frac{\rho_0(y)}{\varepsilon_0 B}. \quad (1)$$

Integrating the last relation within the beam depth, we obtain

$$\Delta v_0 = v_0 \left( y_0 + \frac{\Delta}{2} \right) - v_0 \left( y_0 - \frac{\Delta}{2} \right) = \frac{\omega_p^2 \Delta}{\omega_c}, \quad (2)$$

where  $\omega_p^2 = ((e/m)\bar{\rho}_0)/\varepsilon_0$ ,  $\omega_c = (e/m)B$  is the cyclotron frequency,  $y_0$  is the transverse coordinate of the beam axis, and  $\bar{\rho}_0$  is expressed as

$$\bar{\rho}_0 = \frac{1}{\Delta} \int_{y_0 - \frac{\Delta}{2}}^{y_0 + \frac{\Delta}{2}} \rho_0(y) dy.$$

The main conclusion is that a thick beam has different velocities of the electrons on its boundaries, namely  $\Delta v_0/v_0 = (\omega_p^2 \beta_e \Delta)/(\omega \omega_c)$ , where  $v_0$  is the velocity of electrons on the beam axis,  $\beta_e = \omega/v_0$ . If  $\rho_0(y) = \text{const} = \rho_0$ , than from the equation (1) we find that the beam has a linear distribution over speeds

$$v_0(y) = v_0 + \frac{\omega_0^2 (y - y_0)}{\omega_c}. \quad (3)$$

Let's go to the model of an infinitely thin beam with a surface density  $\sigma_0 = \rho_0 \Delta$ . It's obvious that this beam is a kind of this charged band, on which the field  $E_0$  breaks. From the equation  $\text{div} \vec{E}_0 = \rho/\varepsilon_0$  it follows that

$$E_{02} - E_{01} = \frac{\sigma_0}{\varepsilon_0}, \quad (4)$$

where the indexes 2 and 1 refer to the field values upper and below the beam, respectively. As one can see from the formulas (1)–(3), with  $\Delta \rightarrow 0$  all the beam electrons move with the constant velocity  $v_0 = E_0/B$ . Let's mark that the ratio (2) can be formally obtained from (4), dividing it on  $B$ . If we

put in the plasma frequency  $\Omega_{pl}$ , which refers to infinitely thin beam with finite value of the flowing current, then

$$\frac{\Delta v_0}{v_0} = 2 \frac{\Omega_{pl}^2}{\omega \omega_c}. \quad (5)$$

As it was shown in [13], solution for drifting infinitely thin flow in the case when it is equally distant from conductive planes, is a superposition of two waves with propagation constants

$$\beta_{1,2} = \beta_e \left( 1 \mp j \frac{\Omega_{pl}^2}{\omega \omega_c} \right), \quad (6)$$

one of which ( $\beta_2$ ) increases with spatial coordinate and the other ( $\beta_1$ ) fades (all variables are assumed to change according to the law  $e^{-j\beta x}$ ). Thus, there is instability, which is called diocotron one. The physical process of the emergence and development of instability can be explained as follows. Let's assume that at the entrance to the drift space some pulsations of electron flow take place, so that there are longitudinal  $\tilde{x}$  and transverse  $\tilde{y}$  high frequency (HF) displacements of electrons. Then, as shown in [13], for the simplest geometry, the pulsing electron beam is exposed by HF electric field of the space charge with the components  $\tilde{E}_x = -\omega_{PH} B \tilde{x}$  and  $\tilde{E}_y = \omega_{PH} B \tilde{y}$ , the static electric field ( $\tilde{E}_0 + \tilde{E}_0$ ) and magnetic field ( $B$ ). In adiabatic approximation we have:  $\tilde{v}_x = \tilde{E}_y / B = \omega_{PH} \tilde{y}$  и  $\omega_{PH} = \Omega_{pl}^2 / \omega_c$ . It means that under the influence of the transverse component of the space charge field and static magnetic field, an alternating component of the longitudinal speed  $v_x$ , appears, which leads to longitudinal displacements  $\tilde{x}$  in the beam (Fig. 1, a). A consequence of the longitudinal displacements of electrons is their grouping in space 1-2 (Fig. 1, b) and appearance of longitudinal component of the space charge field  $\tilde{E}_x$ . Then, insofar as  $\tilde{v}_y = -\tilde{E}_x / B = \omega_{PH} \tilde{x}$ , the transverse component of the electron velocity appears, and therefore, additional transverse displacement  $\tilde{y}$  of the beam, which is rather called by initial pulsation. This additional transverse displacement creates an increased component of the space charge field  $\tilde{E}_y$ , and the process described above is repeated.

In the considered model, the number of electrons for which  $\tilde{y} = \tilde{y}_1 > 0$  and the number of electrons for which  $\tilde{y} = \tilde{y}_2 < 0$ , are equal, and  $|\tilde{y}_2| = |\tilde{y}_1|$ , thus, if there is no constant component of the space charge field, the risen electrons will give to the field  $\tilde{E}_0$  as much energy as the descending ones will take. But from formula (4) it follows that the static field under the beam is less than above the beam, because of the action of the constant component of the space charge field. Due to this, when

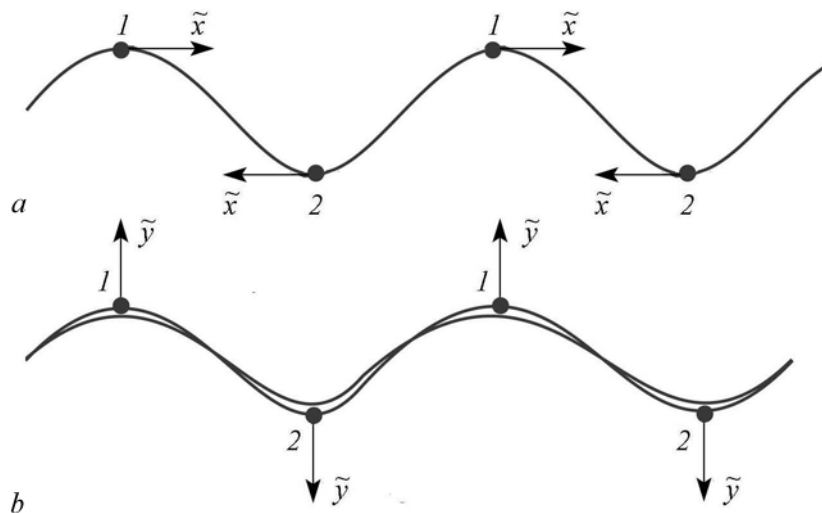


Fig. 1. Evolution of diocotron instability

$\tilde{y} > 0$  the beam gives more energy than it takes when  $\tilde{y} < 0$ . In other words, the RF energy source is the constant component of the space charge field, which leads to different values of the field on different sides of the plane  $y_0$  of the equilibrium position of the beam.

One of the main results of the study of hydrodynamic instability of electron beams [7, 8] is that two-dimensional vortex flow of an ideal incompressible fluid and two-dimensional motion of electrons across a sufficiently strong magnetic field, even within the framework of nonlinear theory, are described by the same equations up to terms, which are inversely proportional to the squared cyclotron frequency, which should be much larger than all other frequencies. This result allows us to interpret the diocotron instability of electron flows in crossed fields as well-known Kelvin–Helmholtz hydrodynamic instability (instability of vortex flows of incompressible fluids). Instability of thick electron beams in crossed fields is explained by sliding electron layers relative to each other [9, 10, 15] and is called slipping instability<sup>1</sup>. For the occurrence of such instability, the layers must slide parallel to the surface layer of the beam. Insofar as the magnitude of the electric field is not the same in different longitudinal cross sections of the flow, the electrons drift velocity also changes, which leads to the slip of the layers. In the framework of linear theory the instability is explained by interaction of two surface waves at beam boundaries [15], allowing to speak about connection of slipping instability with instability of vortex surfaces in hydrodynamics [16]. Formally, a speed shift can be introduced into the theory of infinitely thin beam using formula (5). Substituting it into expression (6) for propagation constants of diocotron waves, we find

$$\beta_{1,2} = \beta_e \left( 1 \mp j \frac{\Delta v_0}{v_0} \right), \quad (7)$$

Which is true for  $\Delta v_0/v_0 \ll 1$  and coincides with the corresponding relations of the theory proceeding from the model of a beam with finite thickness. Let's note, as it follows from relation (7),  $\beta_{1,2}$  depend on  $\Delta v_0$  for any beam thickness.

There are also the results of computer experiments investigating the described instabilities, from which the work [6] is standing out. This work presents footage from a short film on the evolution instability of an electron beam in crossed fields at different points in time. Here we can add the results of Ph.D. thesis [12] and [17]. In our opinion, of particular interest is the work [11], which in the reasons of dimension shows that, in the framework of the two-dimensional model, the development of turbulent perturbations leads to the expansion of an electron beam across the magnetic field, proportional to the distance in the drift space and that the noises of turbulent origin have a maximum at a certain frequency, which is back proportional to this distance.

The importance of this work is due to the fact that it considers the statistical characteristics of the turbulent motion of electrons, which are obtained by averaging the corresponding values over the time and the statistical ensemble. In particular, an analogue of the Schottky formula for turbulent noise is obtained.

For the mean square of current fluctuations due to spectral components from the frequency range  $\Delta\omega$ , the following formula is obtained:

$$\overline{(\Delta I)_\omega^2} = I_0^2 \frac{\sigma_0 x}{\varepsilon_0 E_0 v_0} \varphi \left( \frac{\sigma_0 x}{\varepsilon_0 E_0 v_0} \right) \Delta\omega, \quad (8)$$

where  $\sigma_0$  is the mean charge per unit of beam square,  $\varepsilon_0$  is the dielectric constant,  $E_0$  is the constant electric field,  $v_0 = E_0/B_0$ ,  $B_0$  is the magnetic field induction,  $I_0$  is the constant component of current,  $x$  is the longitudinal coordinate.

<sup>1</sup>The results of analysis of space charge waves in electron beams in crossed fields are set out in monograph [13, Ch. 5] (see also the bibliography in this monograph and in [10]).

According to numerical experiments [6] and the hydrodynamic analogy [7] in the beam cross section, where its width  $\overline{\Delta y} = CUt$ ,  $C$  is the dimensionless coefficient,  $U = \sigma_0/(\varepsilon_0 B)$ , there predominantly formed clusters with the size  $\sim \overline{\Delta y}$ , following each other with the interval  $\sim 2\overline{\Delta y}$ . Therefore, the noise in this section should be maximum at

$$\omega = \omega_{\max} \sim \frac{\pi v_0}{\overline{\Delta y}} \sim 12 \frac{v_0 \varepsilon_0 E_0}{\sigma_0 x}, \quad (9)$$

Where it is assumed that  $C \sim 0.25$ . Supposing  $\omega \ll \omega_{\max}$ , and  $\varphi(\xi) = C_0 + C_2 \xi^2$ , the author [6] obtains the formula

$$\overline{(\Delta I)_\omega^2} \approx I_0^2 \frac{\sigma_0 x}{\varepsilon_0 E_0 v_0} \left[ C_0 + C_2 \left( \frac{\sigma_0 \omega x}{\varepsilon_0 E_0 v_0} \right)^2 \right] \Delta \omega, \quad (10)$$

where, for physical reasons,  $C_0 > 0$  and  $C_2 > 0$ .

It is shown above that the third group of works considers swirl turbulence, although it would be more correct to speak of turbulence associated with the formation of coherent structures in an electron beam and their interaction [17–19]. When slipping instability appears, then filamentization of the beam may take place. The similar model is studied in [17] and represents a stream of charged filaments in a uniform magnetic field. Numerical experiments showed that the greater is the amplitude of the perturbations, the greater is the number of filaments involved in the interaction, and the denser they are arranged, then the faster and more intense is the intersection of filaments and formation of swirl structures, which leads to turbulence. Swirls are very important in drift turbulence in plasma [20]. Propagating in plasma, swirl structures carry part of the substance in the form trapped particles, which can strongly effect on transport processes and cause noticeable density fluctuations. Random position and phase of the vortex structures due to collisions between them, which allows to construct a model of plasma turbulence as an ensemble of drift vortex structures, placing vortices of various amplitudes randomly in space [20].

There are many works, devoted to plasma and beams vortexing (see, for example, [21–24] and their bibliography). Most of the works speaks about the occurrence of isolated vortices. For example, the work [23] theoretically proves the possibility of existence of nonlinear stationary waves of the type localized vortices, in electron beams, heterogeneous in density and (or) in speed, moving along a constant magnetic field. As it is shown, the vortex as a whole has a spiral structure rotating around the axis of the beam. Authors express the assumption that such vortices in electron flows can occur either under the action of appropriate external influences, or due to the developed instabilities: slipping instability in continuous beams and diocotron instability in tube beams. The works [21] and [22] also consider vortex dynamics in electron beams, moreover these papers contain not only theoretical, but also experimental results. However, these works study only isolated vortices, while in [22] the interaction of pairs of them is considered. All the works devoted to vortices mention their bonding only like this: with the development of diocotron instability, large vortices break up into smaller vortex structures, nonlinearly interacting with each other. Thus, by this day there are no analytical theory of vortex turbulence. Moreover, in respect with vortex turbulence, the opinion of hydrodynamicists is interesting, which we cite here from [25, p. 373–374]: “In a turbulent flow an actually steady motion of the medium is steady only for time-average values of speed and pressure, while instantaneous values of speed and pressure, has irregular ripples. The term “turbulence” is often used quite in a free way. Thus, any complex swirling or unstable movement may be called a turbulent flow. But researches, working with turbulent flows, have a very definite concept of this subject. Any motion, which can be describes as periodical one, or which represents a correct vortex model (to some extent), is not a turbulent flow, no matter how complex it is. Essential characteristic of turbulent flow is that the turbulent pulses are chaotic by its nature. Therefore, complete and logical consistent solution of turbulence problem requires application of methods of statistical mechanics”. The last became unobvious after the discovery of dynamical chaos.

## 2. Turbulent electron beams and generators based on them: experimental results and phenomenological models [21–29]

The formation of turbulent electron beams can be carried out using electrostatic fields and space charge fields, magnetostatic fields and space charge fields, combined electro- and magnetic fields and space charge fields. The principal property of turbulent flows is the formation of space charge clots, which are interacting with each other, leading to complex dynamics of the beam generating noise-like fluctuations. Then there can be offered a phenomenological description of such beam as an ensemble of interacting structures consisting of classical nonlinear oscillating and self-oscillating elements. The works [26–30] consider different schemes of noise-like generators, in which differently formed turbulent electron beams are used. All experimental layouts have a common structure. It contains the sections of: electron gun; control electrodes; section of electron beam transformation; electrodynamical amplification system with power input and output, and a collector. Let's study the turbulent beam properties in dependence of their forming methods, and the devices, in which they are used, according to the works [26–30].

**2.1. Of turbulent electron beams formed by magnetron injection guns and of generators based on them.** Devices, using magnetron injection guns (MIG), always demonstrate high noise level. Earlier most of the research was aimed at reducing abnormally high noise in such devices in every

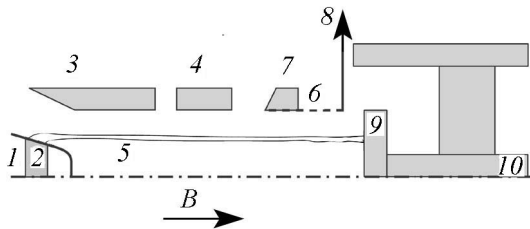


Fig. 2. The scheme of the magnetron-injection gun: 1 – cathode, 2 – emitting belt, 3 – controlling electrode, 4 – anode, 5 – electron beam, 6 – spiral cut, 7 – absorbing piece, 8 – energy output, 9 – high-frequency probe (collector), 10 – center conductor of the HF probe [27]

possible way. Currently in connection with the emergence of new methods of information transmitting, radiolocation, as well the needs of manufacturing industry, noise-like broadband signals acquire a number of important applied appointments. In this regard, we present the results of experimental study of beam structure and output characteristics of generators with MIG, which form turbulent electron beams near the output of gun section [27].

The object of study in [27] is the layout of MIG (Fig. 2), which used conical cathode with emitting metalloporous thermobelt of 1–3 mm width, control electrodes and anode. The layout has the possibility of longitudinal and transverse moving of magnetic focusing system.

The studies of dependence of beam structure, formed by MIG, output integral power and generation band from magnetic field value was made. The results shown in Fig. 3 and Fig. 4, were obtained for thermobelt width 1 mm. In figure 3 one can see the distribution of maximum density of current through the span channel, measured for different values of magnetic field. With some values of magnetic field one can see increasing of maximum current density and some oscillations of this value through the span channel. This indicates that some intense bunches of spatial charge are forming in the beam. In Fig. 4 one can see the distribution of space charge density in beam cross section at the distance from the cathode equal to 4 mm. The figure demonstrates azimuthal heterogeneity of the electron beam, which it acquires almost at the exit of gun section.

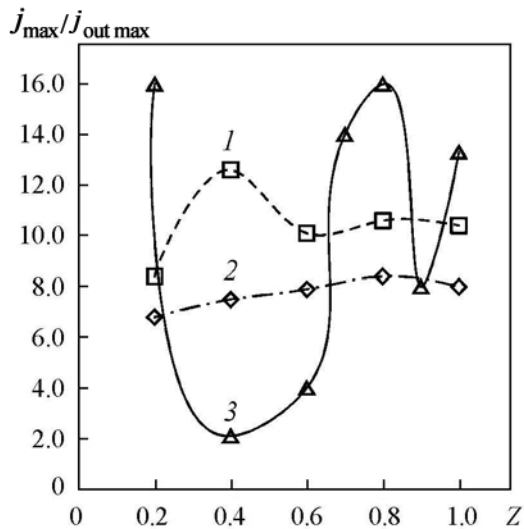


Fig. 3. Change of maximum beam current density along the drift length depending on the magnitude of the magnetic field value  $B$ : 1 – 0.04 T, 2 – 0.02 T, 3 – 0.056 T [27]

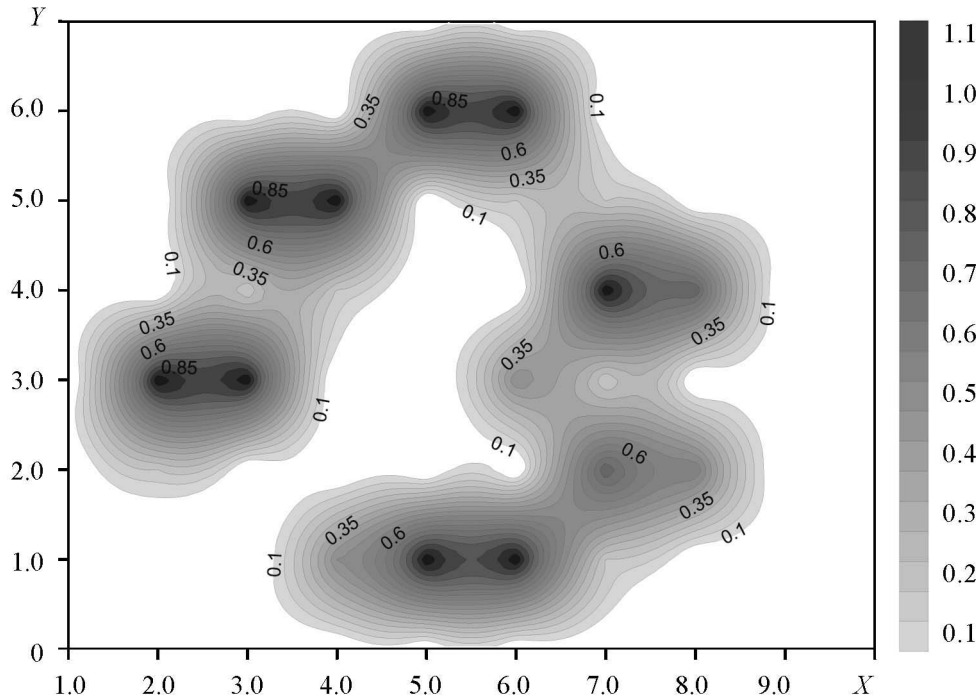


Fig. 4. Qualitative image in dimensionless coordinates  $(X, Y)$  of electron bunches in the beam cross section at a distance 4 mm from the cathode. Space charge density is shown in grayscale (in dimensionless units). The graduation scale is shown to the right of the figure [27]

The analysis of Fig. 3 and 4 shows that in the systems with MIG one can find the forming of interacting space charge bunches not only on the plain  $(r, z)$ , but also in the plain  $(r, \varphi)$  (here  $z$  is the longitudinal,  $r$  is the transverse,  $\varphi$  is the azimuthal coordinates). Thus, the electron beam in MIG systems is fundamentally turbulent, what is connected with the features of its formation in the gun section. We can suppose, that such heterogeneity of the electron beam generated by MIG is associated with different characteristics of electron groups, emitted from different ends of cathode thermobelt, which acquire velocities, different by modulus and direction.

Thus, there is some stratification of the electron beam: speed and direction of emitted electrons will depend on which part of the thermobelt they were emitted by. The difference in the characteristics of emitted electrons (direction of their speed and speed modulus) will increase if the width of the emitting thermobelt enlarges. The last should lead to an even greater increase of inhomogeneities in the electron beam, to its even stratification. Table 1 presents data characterizing the dependence of current density and quantity of space charge clusters from the width of the emitting thermobelt. The analysis of the obtained experimental data shows that as the width of the thermobelt increases, both the density of the current, and the number of space charge clusters enlarge.

In other words, turbulence of an electron beam manifests itself the more, the greater is the width  $h$  of the emitting cathode thermobelt. In the drift space such beam becomes strongly non-laminar, which leads to appearance of many space charge clusters.

Table 1

Dependence of the normalized density of current  $j_{\max}/j_0$  and the number of space charge bunches  $N$  from the width  $h$  of cathode thermobelt,  $j_0$  is the initial density of current

$h$ , mm	$j_{\max}/j_0$	$N$
1	6	34
2	14	112
3	22	184



Examination of experimental study of output characteristics of generators with MIG showed that the width of the thermobelt significantly affects on the characteristics of the generated signals: with increasing width of the thermobelt, one can see increase of power and bandwidth of generated signals, as well as increasing of maximum frequency of generation. Besides, with the increase of thermobelt width the power drop in the output signal spectrum decreases. The result is due to the fact that with an increase of the width of the emitting thermobelt, there increases as the current density, so as the quantity of space charge clusters (see Tab.1), spatio-temporal fluctuations of which become the sources of powerful broadband microwave noise. Thus, we make a conclusion that MIG generators have significant advantage over other similar devices, as they allow to obtain quite powerful broadband noise-like microwave oscillations. The reasons for such abnormally high noise level in MIG generators, according to [26], are: the formation of space charge clusters in the planes  $(r, z)$  and  $(r, \varphi)$ ; the beam formed by MIG consists of different layers of electrons (beam stratification) having different characteristics (modulus and direction of speed, density, etc.)

**2.2. Generator of broadband noise-like microwave oscillations with a turbulent electron beam.** In the work [28] it is assumed that the electron beam is axially symmetric. In the theoretical model, the electron flow is divided into  $N$  charged layers with a depth  $dr$  embedded in each other, each of which is replaced by an infinitely thin charged cylinder. To each cylinder current  $I_j$  is assigned. The motion equations for  $j$ th charged cylinder in cylindric coordinates are the following:

$$\frac{d^2 r_j}{dt^2} - r_j \left( \frac{d\varphi}{dt} \right)^2 = -\eta E_{r,j} - \eta \left( r_j \frac{d\varphi}{dt} B_{z,j} \right),$$

$$\frac{d^2 z}{dt^2} = -\eta E_{r,j} - \eta \left( r_j \frac{d\varphi}{dt} B_{r,j} \right),$$

$$j = 1, 2, \dots, N,$$

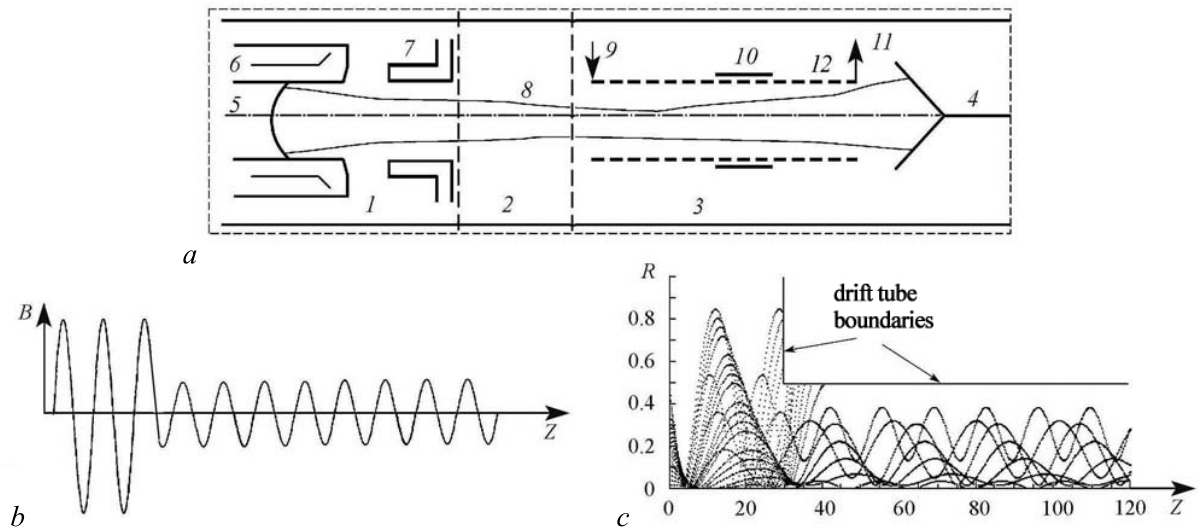


Fig. 5. *a* – schematic diagram of a generator of broadband noise-like fluctuations: 1 – electron gun section; 2 – beam transformation section; 3 – amplification section; 4 – collector; 5 – cathode; 6 – system of electrodes; 7 – anode; 8 – electron beam; 9 – energy input; 10 – absorber; 11 – energy output (energy puller); 12 – electrodynamic amplification system; *b* – distribution of the magnetic field along the generator axis, *c* – trajectories of electrons passing through the transformations section and amplification section in an inhomogeneous magnetic field [28]

where  $z, r, \varphi$  are the longitudinal, transverse and azimuthal coordinates of  $j$ th cylinder, respectively,  $\eta = e/m$  is the specific charge of an electron,  $e$  is the electron charge,  $m$  is the electron mass,  $E_{rj,zj}$  is the space charge field strength at a point with coordinate  $(r_j, z_j)$ ,  $B_{rj,zj}$  is the magnetic field induction at a point with a coordinate  $(r_j, z_j)$ . Since the strength of space charge field of the  $j$ th charged cylinder is

$$e_j = \frac{I_j}{2\pi\epsilon_0\sqrt{2\eta}U^{\frac{1}{2}}r} \quad \text{with } r \leq r_j, \quad e_j = 0 \quad \text{with } r \geq r_j,$$

where  $I_j$  is the current of the  $j$ th charged cylinder,  $\epsilon_0$  is the dielectric constant,  $U$  is the accelerating voltage, the total strength of the space charge field has the form

$$E_{rj}(r) = \sum_{j=1}^N e_j(r_j).$$

In the studied construction (traveling wave tube – amplifier) the three areas are distinguished (see Fig. 5, *a*). They are: the area of laminar beam formation (electron gun) 1, the area of transformation a laminar beam to a turbulent one (electron beam modulator) 2, amplification area 3. An electron beam in a generator comes into transformation area with periodic magnetic field, which makes space charge clusters in a beam. Microwave oscillations arising in this section come to amplification section. In Fig. 5 one can also see the results of theoretical study of a broadband noise-like microwave generator with turbulent electron beam. In Fig. 5, *b* one can track the action of strong magnetic field upon an electron beam. In Fig. 5, *c* we show electron trajectories in dimensionless coordinates. It is clearly seen that in the beam there are areas of strong compression and intersection of trajectories, and that in intense turbulent electron beam there occur space charge clusters. The emergence of space charge clusters can due to both an increase of current density and the change in the longitudinal velocity of electrons. The latter is connected either with electron deceleration, or with an increase of the transverse and azimuthal constituents of electron velocities.

In Fig. 6 in grayscale the normalized space charge density  $\rho/\rho_0$  distributions are presented (here  $\rho_0$  is the initial space charge density) in turbulent electron beam for different values of magnetic focusing, characterized by the parameter  $\alpha = 2 \cdot 10^8 (B_0^2 L^2)/U$  (here  $B_0$  is the magnetic field amplitude,  $L$  is the magnetic field period,  $U$  is the accelerating voltage), which depends from the amplitude and period of magnetic field. White areas in the picture correspond to the normalized space charge density less than 1, and black areas correspond to its maximum value. Changes in the value of  $\alpha$  were carried

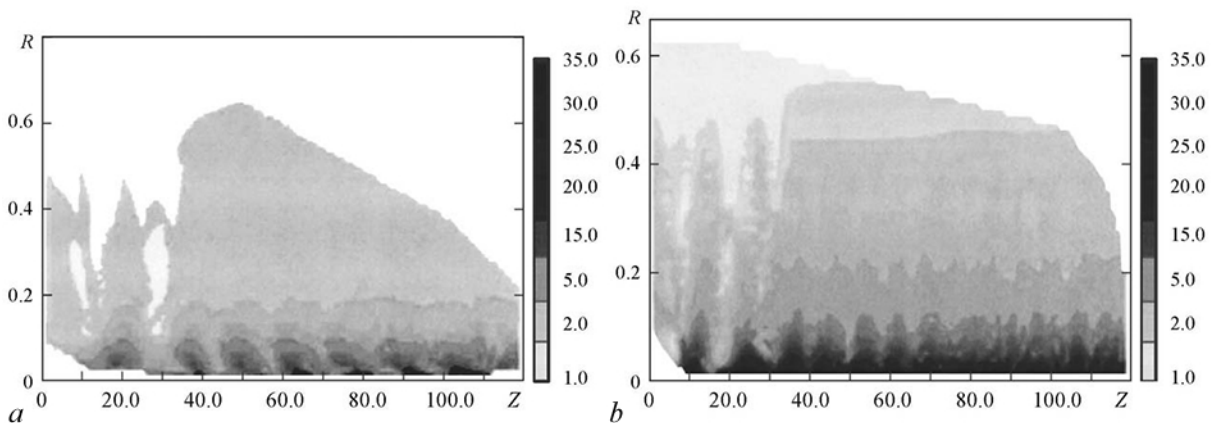


Fig. 6. Distribution (in grayscale) of normalized space charge beam density along the radius and longitudinal coordinate for various values of the magnetic focus parameter  $\alpha$ : *a* – 0.2, *b* – 3.0 [28]

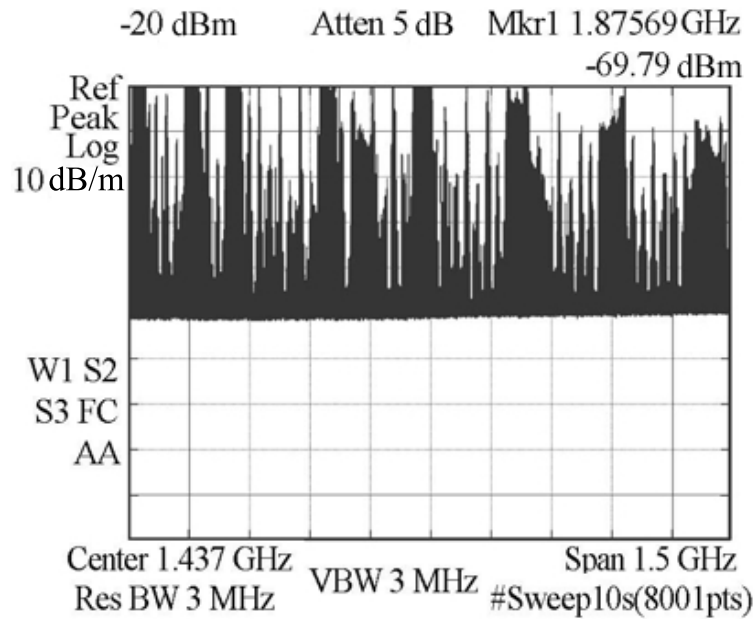


Fig. 7. The spectrum of noise-like microwave oscillations obtained at experimental research [28]

out by increasing the magnetic field amplitude. For  $\alpha = 3$  in space charge density distribution one can observe significantly more (than with  $\alpha = 0.2$ ) regions/ where  $\rho/\rho_0$  has maximal value. In Fig. 7 we represent characteristic spectrum of chaotic oscillations for  $\alpha = 3$ .

**2.3. Electrically tunable generator of broadband chaotic microwave oscillations with turbulent electron beam.** Electrically tunable generator of broadband chaotic microwave oscillations with turbulent electron beam also allows to obtain high output characteristics [29]. The scheme of this generator is presented in Fig. 8, *a*. The principle of operation of the generator is as follows. An electron beam is formed by an electron gun. It is injected into modulation section, where it becomes turbulent under the affect of inhomogeneous magnetic field (Fig. 8, *b*) and decelerating electric field (Fig. 8, *c*). The beam becomes consisting in length of individual clusters of space charge. A braking electric field is created by applying voltage  $U_{eds} < U_0$  (here  $U_{eds}$  is the potential on electro-dynamical amplifying system (EDAS),  $U_0$  is the anode accelerating system). The modulated electron beam enters the EDAS region, where it is amplified. From the EDAS region, the spent beam enters the collector. The output signal is taken from the amplifier through the output of energy. The generation mode in the device is regulated by changing the EDAS potential  $U_{eds}$ .

Under the influence of a strong magnetic field, the space charge density in some regions of the beam is 50–70 times higher than the initial value, which leads to forming of isolated clusters (electron groups), instable in time and space. A moving grouped intense electron beam has a power that, during its deceleration, turns into radiation.

According to the results of numerical simulation, the number of space charge bunches was calculated at various values of the beam braking coefficient  $K$ , which was defined as follows:

$$K = 1 - \frac{U_{eds}}{U_0}.$$

We took into account the clusters, which space charge density  $\rho$  was larger than initial density  $\rho_0$ . During numerical experiments it was found that with low braking  $K = 0.4$  (Fig. 9, *a*) the distribution of the number of space charge clusters has a well-expressed maximum. For large values of the braking

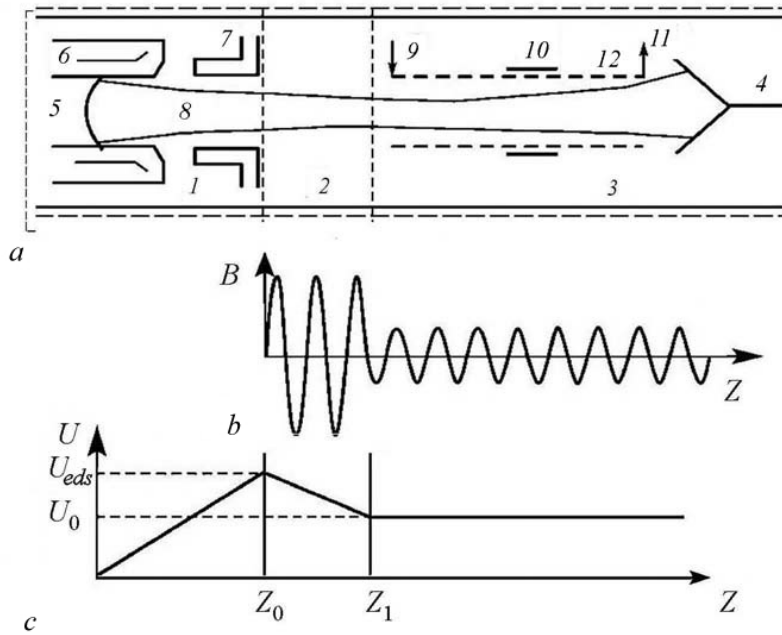


Fig. 8. *a* – schematic diagram of an electrically tunable generator of chaotic oscillations: 1 – electron gun section, 2 – electron beam modulation section, 3 – amplification section, 4 – collector, 5 – cathode, 6 – system of electrodes, 7 – anode, 8 – electron beam, 9 – energy input, 10 – absorber, 11 – energy output (energy puller), 12 – electrodynamic amplification system; *b* – distribution of the magnetic field  $B(z)$ ; *c* – distribution of potential  $U(z)$  [29]

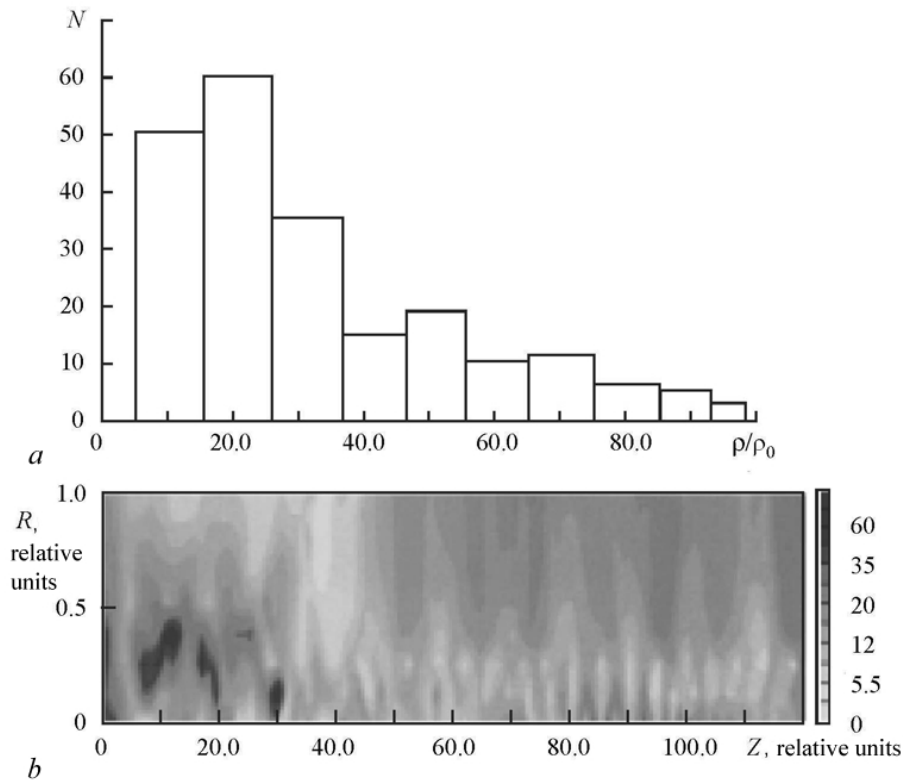


Fig. 9. Results of numerical modelling: *a* – distribution of the number of space charge bunches for  $K = 0.4$ , *b* – distribution of the space charge density  $\rho_0(R, z)$  of the beam for  $K = 0.4$  [29]

coefficient  $K$  the distribution of the clusters number is more uniform, without expressed highs. In Fig. 9,  $b$  the space charge density in the weak braking regime ( $K = 0.4$ ) is presented. The most dark areas correspond to space charge density, 70 times larger than the initial value.

The study showed that the formation of turbulent electron beams can be carried out by either a significant increase of the magnetic field amplitude, or through the use of a combination of a small magnetic field and a braking electric field. The last case is preferred, because in this case, as shown by numerical simulation, the current flow in the system is higher.

The dependence of the output power  $P$  on the magnitude of the braking coefficient of the electron beam  $K$  is shown in Fig. 10,  $a$ , (curve 2). From the figure it is clearly seen that the dependence  $P(K)$  has areas of rise and fall. The decline of output power is due to the fact that clusters of space charge at large values of  $K$  become less dense, as the current subsidence on the EMF increases. Dependencies of the electron (curve 3) and technical efficiency (curve 1) from the potential of the EMF also have rise and fall regions. With an increase in the inhibitory potential, the band of generated frequencies increases (Fig. 10,  $b$ , curve 2), which is connected with the appearance of many space charge clusters. The experimentally measured dependence of the current flow on the braking coefficient of the electron beam  $K$  is shown in Fig. 10,  $b$  (curve 1). One can see that with an increase of  $K$ , current subsidence increases, which leads to a decrease in the generated power output (see Fig. 10,  $a$ , curve 2).

Thus, the mode of generated oscillations can be controlled by changing the braking potential – the potential on the EMF.

Currently, the relevance of the development, creation and research of chaotic broadband microwave radiation sources is due not only to classical tasks of radio countermeasures and radio suppression, but also by the presence of a number of interesting practical applications of chaotic signals in information transmission systems based on dynamic chaos, in noise radar systems, in the manufacturing industry [30]. A distinctive feature of devices, the principle of operation of which is based on the use of turbulent electron beams, is that it's possible to transform the industrially produced devices (for example, TWT) by changing the transition region of a periodic magnetic field into a chaotic oscillation generator [26].

Summarizing all written above, we can state that the experimental results of [26–30] are related at a qualitative level to various scenarios of the appearance of coherent self-sustaining electronic structures in the electron beam and their interaction.

It should be noted that often the emergence and development of dynamical chaos regimes is called turbulence. In our opinion, the identification of these phenomena requires justification in each specific case. As it follows from the previous statement, there is no overall picture of the emergence and development of turbulence in electron flows, not to mention the theory. Therefore it still seems relevant to be conducting special practical experiments and constructing phenomenological models

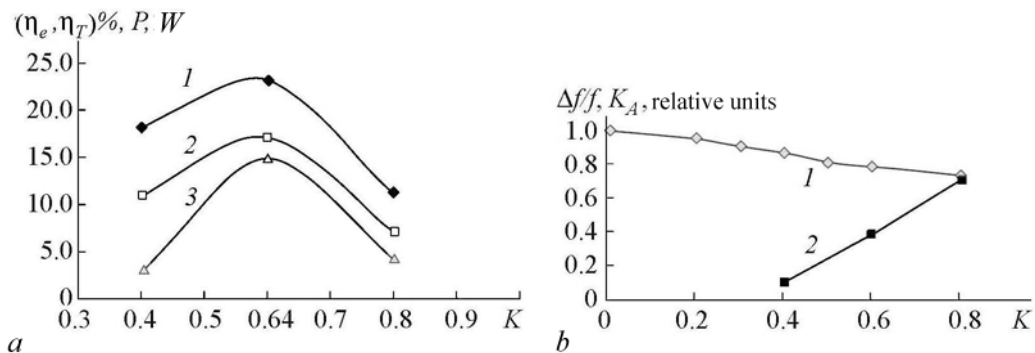


Fig. 10. Results of experimental study:  $a$  – dependence of technical efficiency  $\eta$  (curve 1), output power  $P$  (curve 2) and electron efficiency  $\eta$  (curve 3) from the beam braking coefficient  $K$ ;  $b$  – dependence of current flow value  $K_t$  (curve 1) and generation bandwidth (curve 2) from the beam braking coefficient  $K$  [29]

based on them. Of particular interest are «composed» chain models consisting from classical oscillatory elements interacting with each other. For example, [31] discusses interacting small volumes of an active medium consisting of electrons-oscillators. Assuming that for each element of such a system, there exists a cooperative radiation, arising, as it is known, due to interactions of electron through the field of their self-radiation, which is phasing for them. Such processes can occur only in systems of nonlinear, non-isochronous oscillators – precisely, the phasing occurs because of non-isochronous. It is shown that when combined superradiant bunches are combined in a chain, then in a system chaotic dynamics can be over time established.

An attempt to combine experiment with calculations within phenomenological model is undertaken in the work [32]. Experimental studies were conducted using soldered layout of a system with electron feedback –turbulent electron beam generator (TEBG). Formation of dense electron structures in drift space of the studied system (due to additional braking of the electron beam by the collector potential) allows considering of this system as a model for the study of turbulent electron beams. The schematic diagram of laboratory layout of TEBG is shown in Fig. 11. The power supply of the laboratory layout was carried out continuously, using several power sources. The main parameters that control the dynamics of the investigated system with turbulent electron beam, are: accelerating voltage (potential difference at the first anode); collector voltage, which is inhibitory to electron beam emitted from the cathode; potential difference on the control electrode and potential difference at the second anode. In the experimental study, the following control parameters were used: accelerating voltage at the first anode  $U_0 = 1200$  V, collector potential relative to cathode  $\Delta U_k = 100$  V (the cathode potential was taken as 0). Preliminary experiments found that potential difference at the control electrode has a significant influence on the formation of higher harmonics in the output spectrum of the low-voltage TEBG. Respectively the potential difference at the second anode did not change and was selected equal to  $\Delta U_2 = 830$  V. Potential on the control electrode relative to the cathode varied in the range  $U_{cont} = -190 \dots -40$  V.

As a result of experimental studies, it was found that with a decrease of potential on the control electrode to -40 V one can observe the forming if higher harmonic components. The maximum generation frequency was 5.52 GHz, which corresponds to the 13th harmonic of basic generation frequency (Fig. 12). Thus, [32] experimentally showed the formation of higher harmonic components in the spectrum of the output signal of the laboratory layout of TEBG with electron feedback, which demonstrates the fundamental possibility of generation in the shortwave microwave range.

As mentioned above, the experimental studies found that in low-voltage vacuum generators with electron feedback there arise structures in electron beams in drift space – dense electron self-sustaining bunches, between which there is a transfer of energy [26–30]. In some cases, bunches had vortex structure, which was the basis for the phenomenological model, which is a system of interacting «electronic vortices»,

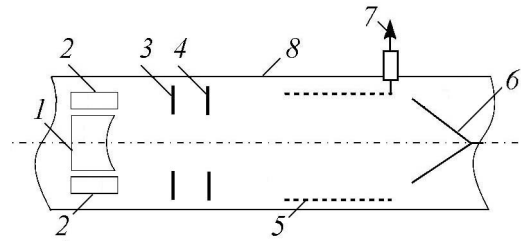


Fig. 11. The schematic diagram of soldered layout of low-voltage TEBG; 1 – cathode, 2 – controlling electrode, 3 – the first anode, 4 – the second anode, 5– a piece of spiral retarding system, 6 – collector, 7 – coaxial broadband microwave output, 8 – drift tube, [32]

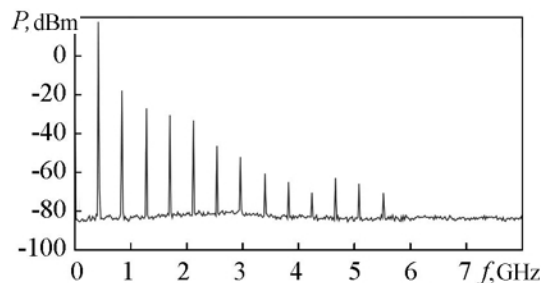


Fig. 12. Experimentally obtained power spectrum  $P(f)$  of output signal of low-voltage TEBG in offline mode [32]

each of them is described by a rough model of tropical cyclone, proposed in the work [33]. From the position of oscillation theory, the dynamics of cyclone-spiral formation around the vertical axis can be interpreted as volumetric self-oscillating process tending to a limit cycle. Such a process can be formally described [32, 33] using two modified van der Pol nonlinear differential equations, defining the dynamics of such local oscillator.

$$\begin{aligned} \frac{d^2 x_i}{dt^2} - a_1(1 - a_2 x_i^2) \exp(-\alpha t) \frac{dx_i}{dt} + \Omega x_i &= 0, \\ \frac{d^2 y_i}{dt^2} - a_3(1 - a_4 y_i^2) \exp(-\beta t) \frac{dy_i}{dt} + y_i &= 0, \end{aligned} \quad (11)$$

where  $\alpha, \beta$  are the coefficients, responsible for the compression or expansion of the vortex, and  $a_1, a_2, a_3, a_4, \Omega$  are the parameters that are set numerically.

Equations (11) reflect the dynamic process for each «particle» of the medium under study. Thus, it was suggested in advance that bunches are peculiar self-oscillating systems. Analysis of equations (11) shows that it is possible to change the development of a self-oscillating process in a system by gradual change of parameter  $\alpha$  ( $\alpha > 0$ ). In this case, due to the gradual increase of  $\alpha$ , the compression of the «bunch» occurs.

To study the processes in a chain of vortices, we used the system of two modified nonlinear differential van der Pol equations of the following kind [32]:

$$\begin{aligned} \frac{d^2 x_i}{dt^2} - a_1(1 - a_2 x_i^2) \exp(-\alpha t) \frac{dx_i}{dt} + \Omega x_i + K_B x_{i+1} &= 0, \\ \frac{d^2 y_i}{dt^2} - a_3(1 - a_4 y_i^2) \exp(-\beta t) \frac{dy_i}{dt} + y_i + K_F y_{i-1} + K_B y_{i+1} &= 0, \end{aligned}$$

where  $i$  is the number of structure,  $K_F$  and  $K_B$  are the coefficients of mutual influence of structures. The chain consisted of 7 structures (note that the number of combined structures is unprincipled). In the case when each element is affected only by the previous structure, the coefficient  $K_F$  is equal to zero. It was also assumed that  $K_B = 0.5$ . Numerical modeling showed that with an increase in the number of structures in a chain, the number of the spectrum harmonics increases.

Further, in [32], a chain of 7 interacting «electronic vortices» is considered, with the condition that the system is under external influence. In this case, the authors used a modified van der Pol nonlinear differential equation with external influence

$$\begin{aligned} \frac{d^2 x_i}{dt^2} - a_1(1 - a_2 x_i^2) \exp(-\alpha t) \frac{dx_i}{dt} + \Omega x_i + \\ + K_B x_{i+1} = A \cos(\omega t), \end{aligned}$$

where  $i$  is the structure number,  $A$  is the external amplitude,  $K_B$  are the coefficients of mutual interaction of the structures,  $\omega$  in the frequency of external influence. The values of the parameters:  $K_B = 1.2, a_1 = 0.2, a_2 = 0.02, a_3 = 0.2, a_4 = 0.02, \Omega = 1.08, A = 1, \omega = 0.45$ . In Fig. 13 the oscillation spectrum for the seven structure is presented. It can be seen from the figure that 8 harmonics are excited in the system.

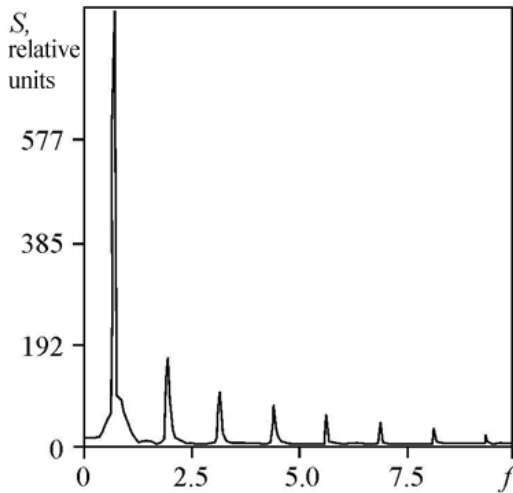


Fig. 13. Spectrum  $S_f$ , obtained by numerical modeling of a chain of structures ( $i=7$ ) described by modified van der Pol nonlinear differential equations [32]

From numerical simulation it was found that with the increasing of structure number the amplitude of the base harmonic decreases. It's due to the fact that the amplitude of other spectral components increases. In this case the spectrums demonstrated in Fig. 13, are discrete, as those in Fig. 12. Taking into account the influence of the previous and subsequent structures on each the structure in the chain, does not significantly affect the nature of the spectrum, which, however, is enriched by additional spectral components.

We have investigated the influence of the input power level  $P_{in}$  on output characteristics of the chain, in particular for power  $P_{out}$ . In Fig. 14 there is presented the dependance of the ratio of output signal and input signal powers  $G = P_{out}/P_{in}$  (let's call this ratio – amplification coefficient) from the value of the normalized power of the external signal  $P_{in}/P_0$ , where normalization was carried out by autonomous generation power  $P_0$ . With numerical simulation, an external signal was applied at the frequency of the first harmonic. The result of numerical modeling corresponds to the curve 1 in Fig. 14. At the same time experimental study of the non-autonomous dynamics of TEBG was carried out, in which an external signal was also applied at the first harmonic frequency. The result of experimental measurements of the amplification coefficient of low voltage TEBG system is illustrated by the curve 2 in Fig. 14. One can see the qualitative conformity of the dependances obtained at experimental studies of a low voltage TEBG system and the results of numerical simulation of a chain of interacting «electron vortices» described by modified nonlinear differential van der Pol equations, in case of power external signal close to the power of autonomous generation.

We also point out possible ways (based on self-organization in unstable media) of creating electron bunches, layers, and filaments when an electron beam passes through a plasma. In the monograph [34] (see also [35]) it is shown that more than 50 unstable media in the approximation of long waves, are described by two hydrodynamical equations

$$\begin{aligned} \frac{d\rho_*}{dt} &= -\rho_* \operatorname{div} \vec{v}, \\ \frac{\vec{v}}{dt} &= C_0^2 \operatorname{grad} \rho_*^{1/m}, \end{aligned} \tag{12}$$

where  $\rho_* = \rho/\rho_0$  is the dimensionless density reduced to the undisturbed one;  $t$  is the time;  $\vec{v}$  is the medium velocity;  $m$  is some azimuthal number, and  $C_0^2$  is the square of effective speed of sound. The role of the reduced density can be played by different values. All the unstable media described by the equations (12), are called «quasi-chaplygin media» in the works [34, 35]. S.A. Chaplygin (1869–1942) in his thesis «Of gas flows» studied as example an unusual gas for which pressure  $p$  is inversely proportional to density  $\rho$ , i.e the product  $p\rho = \text{const}$  and gas expansion does not lead to a drop in pressure, as it really happens, but to its growth. Obviously, «Chaplygin gas» is unstable and does not exist in nature itself, but this model with some modifications is useful for examination of many quasi-chaplygin media. For «Chaplygin gas»  $m = -1/2$ .

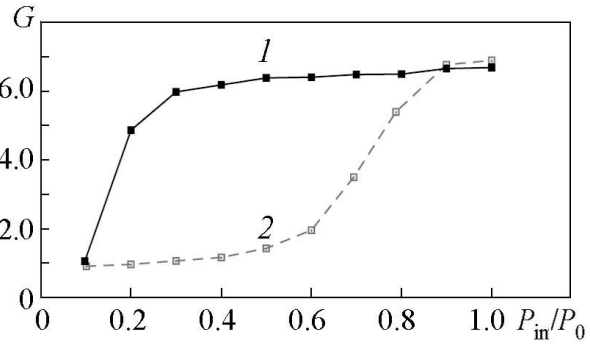


Fig. 14. Dependance of the amplification coefficient  $G$  from the power of the input signal: 1 – the result of numerical modelling of a chain of «vortex structures», 2 – the result of experimental study of low-voltage TEBG [32]



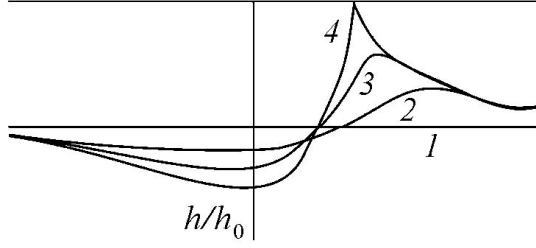


Fig. 15. One of the results of an accurate analytical solution for «drops on the ceiling». The layer is characterized by relative thickness  $h/h_0$  at a given point in the ceiling ( $h_0$  is the initial thickness) [35, Fig. 1, c]

A wonderful illustrative example of the growth of random disturbances, leading to discontinuities in a continuous medium and to the formation of separate bunches, is described in the paper [35, P. 68–69]: «Now imagine that we froze a thin layer of water on the floor, and flipped the whole room upside down, so the ice is on the ceiling, then we instantly heated it, so it turned into a layer of water on the ceiling. It cannot immediately fall down as a whole, since below it is supported by atmospheric air pressure equal to  $1 \text{ kg}\cdot\text{sm}^{-3}$ , but this situation will be unstable, and the layer will begin to gather

in drops and jets falling down. The equations of motion of water in a layer will actually remain the same, but the gravity acceleration will change sign by rule  $g \rightarrow -|g|$ , so the former “tsunami speed” will become imaginary by the transition rule  $c_0 = \sqrt{gH} \rightarrow i\sqrt{|g|H}$ . Such a situation will mean a transition of a stable medium into unstable one. In this medium there will no longer be waves running along the surface, and in the direction perpendicular to it there will grow standing disturbances of a certain «quasi-chaplygin» type, which will lead to the formation of drops and eventually will force all water fall down». In Fig. 15 a variant of an asymmetric drop is presented (a combination of a “hump” with a “dimple”), which grows during time (curves 1–3) up to the complete break of the layer (curve 4).

The monograph [34] with reference to the article [36] sets forth the theory of splitting an electron beam in a cold plasma into bunches. The book considers a plasma of ions and electrons  $e$  penetrated by an electron beam  $E$  and described by equations

$$\begin{aligned} \frac{\partial n_\alpha}{\partial t} + \frac{\partial}{\partial x}(n_\alpha v_\alpha) &= 0, \\ \frac{\partial v_\alpha}{\partial t} + v_\alpha \frac{\partial v_\alpha}{\partial x} &= - \left( \frac{|e|}{m_e} \right) E, \end{aligned} \quad (13)$$

where  $\alpha = e, b$ . It is assumed that the ions are motionless and the quasineutrality condition is satisfied. The system of equations (13) implies the law of current storage in the form:

$$\begin{aligned} n_e v_e + n_b v_b &= n_b^0 v_0 = \text{const}, \\ n_e + n_b &= n_i = \text{const}, \end{aligned} \quad (14)$$

where  $n_b^0$  and  $v_0$  are the initial density and velocity of the beam, which in [34] is called “current uncompensated”. Using (14), equations (13) are reduced to two equations of a more general form than quasi-caplygin equations, namely:

$$\begin{aligned} \frac{\partial \rho_*}{\partial t} + \frac{\partial}{\partial x}(\rho_* v_b) &= 0, \\ \frac{\partial v_b}{\partial t} + v_b \frac{\partial v_b}{\partial x} &= R = \frac{\partial}{\partial x} \left[ \frac{\varepsilon \rho_*}{1 - \varepsilon \rho_*} (\varepsilon v_0 - v_b)^2 \right], \\ \rho_* &= \frac{n_b}{n_b^0}, \quad \varepsilon = \frac{n_b^0}{n_i}. \end{aligned} \quad (15)$$

Taking into account that the perturbations in this model are «drift», the authors of [34] go to a coordinate system moving with the beam, assuming that

$$\begin{aligned}x &= \tilde{x} + v_0 t, \\ \rho_* &= \rho_*(t, \tilde{x}), \\ v_b &= v_0 + v(t, \tilde{x}).\end{aligned}\tag{16}$$

In these variables, the system of equations (15) takes the form

$$\begin{aligned}\frac{\partial \rho_*}{\partial t} + \frac{\partial}{\partial \tilde{x}}(\rho_* v) &= 0, \\ \frac{\partial v}{\partial t} + v \frac{\partial v}{\partial \tilde{x}} &= R = \frac{\partial}{\partial \tilde{x}} \left[ \frac{\varepsilon \rho_*}{1 - \varepsilon \rho_*} (v_0(1 - \varepsilon) + v)^2 \right].\end{aligned}\tag{17}$$

The quasi-chaplygin case takes place under the following conditions:

$$v_0 \gg v, \quad \varepsilon \ll 1,\tag{18}$$

then the right part of (17) becomes equal to

$$R = C_0^2 \frac{\partial \rho_*}{\partial x}, \quad C_0^2 = \varepsilon v_0^2.\tag{19}$$

Thus, the model of plasma penetrated by an electron beam, is equivalent to the capsized shallow water model and can describe a partition of a flow (even without initial push) into clumps, similar to drops on the ceiling. As it is shown in [34], the equations (13) are reduced to quasi-chaplygin equations for  $m = 1$  (similar to those describing drops forming on the ceiling) without any restrictions, if new variables are introduced as:

$$\begin{aligned}n &= n_e - n_b, \\ u &= v_b - v_e, \\ v &= \frac{nu - n_0 v_0}{n_i}, \\ \rho_* &= \frac{n_i^2 - n^2}{n_i^2 - n_0^2} \left( \frac{u}{u_0} \right)^2.\end{aligned}\tag{20}$$

Then there are the following grouping equations:

$$\begin{aligned}\frac{\partial \rho_*}{\partial t} + \frac{\partial}{\partial x}[(v + V_{CH})\rho_*] &= 0, \\ \frac{\partial v}{\partial t} + (v + V_{CH}) \frac{\partial v}{\partial x} &= C_0^2 \frac{\partial \rho_*}{\partial x},\end{aligned}\tag{21}$$

where  $C_0^2 = u_0^2 n_b^0 n_e^0 / n_i^2$  is the velocity, determining the rate of increase at the linear stage of disturbances;  $V_{CH} = (n_b^0 v_e^0 + n_e^0 v_b^0) / n_i$  is the systematic drift rate. If you go into a mobile with a drift rate coordinate system, then the analogy with ceiling drops equations is obvious and corresponds to the dynamics of the «elementary drop», which is by Fig. 15.

The monograph [34] also outlines the solution to the interesting problem of splitting an electron beam in a plasma into layers and filaments. In typical conditions, the beam is long, and therefore, it should not be divided into bunches in the longitudinal direction, but into parallel threads – «filaments». The task is complicated compared to previous, since it is necessary to take into account the magnetic field. The initial equations for the electron beam take the form

$$\begin{aligned}\frac{\partial n_b}{\partial t} + \operatorname{div} n_b \vec{v}_b &= 0, \\ \frac{\partial v_b}{\partial t} + (\vec{v}_b \nabla) \vec{v}_b &= -\frac{|e|}{m_e} (\vec{E} + [\frac{\vec{v}_b}{c} \vec{B}]).\end{aligned}\tag{22}$$

It's assumed that the beam moves along  $x$ , stratifying in the transverse direction along  $y$ , so that the magnetic field has only a component  $B_z$ . Moreover, the fields  $E_y$  and  $B_z$  acting on the beam are excited by the beam itself and are found from the Maxwell equation for the medium. Taking into account some approximations in [34] it is shown that the equations (22) in the coordinate system moving with the flow are reduced to the standard quasi-chaplygin form (as for drops forming on the ceiling) with  $m = +1$

$$\begin{aligned}\frac{\partial \rho_*}{\partial t} + \frac{\partial}{\partial y} (\rho_* v_\perp) &= 0, \\ \frac{\partial v_\perp}{\partial t} + v_\perp \frac{\partial v_\perp}{\partial y} &= C_0^2 \frac{\partial \rho_*}{\partial y},\end{aligned}\tag{23}$$

where  $v_\perp = v_{by}$ ,  $C_0^2 = \varepsilon v_0^2$ ,  $\varepsilon = n_b^0/n_i$ ,  $\rho_* = n_b/n_b^0$ .

The results of an experimental study of the effect of residual gas pressure on amplitude and spectral characteristics of output signal of a turbulent electron beam generator, are given in [37]. The laboratory layout is a device consisting of a cathode, control electrode, anodes, drift tube, movable collector-puller. The last is made in the form of a coaxial line, the central conductor of which is connected to a spiral line segment. The microwave signal is removed from the spiral and fed to a spectrum analyzer. The studies have been made in pulse mode. The paper presents the results of a study of the impact of various factors on generation characteristics and on parameters of space charge bunches. The main results of the work are related to the answer to the question: «What is the effect of residual gas ions on the formation and amplitude of electron bunches?» If the drift tube is filled with low pressure residual gas, then near the bunches there occurs intense gas ionization, due to small electron velocities near them and the potential sag caused by the space charge of the bunch itself. Then the clot is saturated with ions, which leads to its charge neutralization and displacement in collector direction. After reaching the collector generation stops. If the bunch lifetime determined by the ratio [38]

$$\tau \approx \frac{\alpha}{p} \left(1 - \frac{I_{\text{limited}}}{I}\right),$$

is bigger than voltage pulse duration, then gas ionization should not affect the output characteristics of the generator. Here  $p$  is the gas pressure,  $I$  is the beam current in the drift tube,  $I_{\text{limited}}$  is the current limit for a given pipe geometry,  $\alpha$  is a constant, depending from gas type (for the air  $\alpha = 2 \cdot 10^{-10}$ ). Thus, due to charge neutralization, it is possible to form more compact and dense bunches of space charge with longer lifetime. The bunches parameters, obtained experimentally for various values of gas pressure in the drift space, are given in table 2.

As a result of experimental studies, it was found that, at residual gas pressure  $p \sim 10^{-7}$  Torr the bunch formed in the drift space is not dense and blurred along section. The density of bunch current  $j_{\max} = j/j_0 = 12$ . In fact, in this case we have not a single dense clot, but local heterogeneities of current density, each of which contributes to the spectrum signal that becomes noise-like. With increasing the residual gas pressure to a value of the order of  $p \sim 10^{-6}$  Torr, the most intense ionization occurs near bunches, due to low electron velocities in a bunch. Ions weaken the action of Coulomb forces, which leads to a sharp increase of density of bunch current ( $j_{\max} = j/j_0 = 120$ ).

Oscillations of such a dense clot are regular, while the level of the output signal increases significantly (Fig. 16). At a residual gas pressure of the order of  $p \sim 2 \cdot 10^{-5}$  Torr, in the spectrum there appear additional components, corresponding to low-frequency modulation of the main signal, due to natural vibrations of ions. With further increase of pressure up to  $p \sim 6 \cdot 10^{-4}$  Torr and more, the character of modulation complicates. At last, with the pressure  $p \sim 10^{-4}$  Torr and more, one can observe transition to a continuous spectrum, corresponding to the formation of more complex electronic structures in the beam (turbulent nature of the movement). In this case, the spectrum is characterized by weak indentation in the range of several octaves, and noise spectral density is higher than in the case of good vacuum conditions ( $p \sim 10^{-7}$  Torr).

In Fig. 17 one can see the dependence of the ruggedness of the output power spectrum from residual gas pressure. The ruggedness of a noise-like signal is defined as  $\Delta A = \lg P_{\max}/P_{\min}$  (in decibels), i.e. represents ratio of maximum power  $P_{\max}$  to minimum  $P_{\min}$ , which are selected in the operating frequency range  $\Delta f$ . The obtained results indicate that the presence of ion background contributes to a significant improvement in spectral characteristics of the output signal. Thus, with the increase of pressure from  $p \sim 10^{-7}$  Torr to  $p \sim 10^{-3}$  Torr, the roughness decreases from  $\Delta A \sim 40$  dB to  $\Delta A \sim 0.3$  dB, respectively, while the band expands to  $\Delta f \sim 2$  octaves. Earlier in [39], the results of numerical simulation showed that the use of a periodic magnetic field reduces the spectrum cuts to the values of the order of  $\Delta A \sim 15 \dots 18$  dB.

Thus, based on the experimental results presented above, it can be stated that ions have a significant effect on all regimes of the generator with turbulent electron beam. It should be emphasized

Table 2

The dependence of the parameters of space charge bunches from gas pressure in the drift space,  $p$  – gas pressure,  $R$  – transverse size of bunch,  $Z$  – length of bunch,  $j_{\max}/j_0$  – normalized density of current [37]

$p$ , Torr	$R$ , mm	$Z$ , mm	$j_{\max}/j_0$
$5 \cdot 10^{-7}$	0.30	1.20	15
$3 \cdot 10^{-6}$	0.22	0.81	120
$2 \cdot 10^{-5}$	0.10	0.20	190

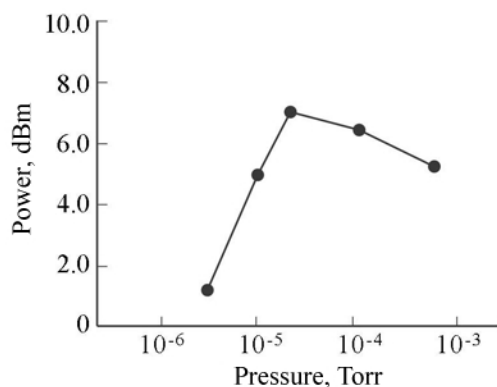


Fig. 16. The dependence of the output power on the pressure of the residual gas, regular mode

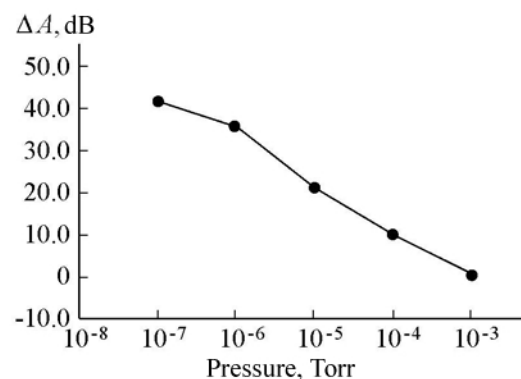


Fig. 17. Dependence of the ruggedness of the output power spectrum from residual gas pressure

that the spectrum of the output signal in the regular regime contains a large number of high order harmonics, which extends the operating range to a shorter wavelength region, and the selection of these components allows in the future to create compact frequency multipliers based on this device.

### Conclusion

The paper presents an overview of the current state of different theoretical approaches to describing turbulence in electron beams. We present the results of experimental study of devices with turbulent electron beams and computational experiment results for a fairly general phenomenological model of interacting electron clots.

There is no general theory of turbulence in electron beams. There is no such theory also in hydrodynamics, although the equation for describing the dynamics of a viscous fluid was formulated long ago. This is the Navier – Stokes equation, the study of which is attributed to one of the seven greatest problems of the millennium. Ian Stuart writes in [40, P. 308]: “The millennium prize problem does not ask mathematicians to find explicit solutions to the Navier-Stokes equation, because this is essentially impossible. Neither is it about numerical methods for solving the equations, important though these are. Instead, it asks for a proof of a basic theoretical property: the existence of solutions.” Maybe in electronics the question should be put like this: does solving of corresponding equations exist for a given state of the electron beam at a certain point in time – with known characteristics of its movement? Stewart ends the article with a link to the Clay Institute website, on which Charles Fefferman wrote: “There are many fascinating problems and conjectures about the behavior of solutions of the Euler and Navier – Stokes equations... Since we don’t even know whether these solutions exist, our understanding is at a very primitive level. Standard methods from PDE appear inadequate to settle the problem. Instead, we probably need some deep, new ideas.”

It seems that such ideas appeared, and their author was Benoit Mandelbrot. In the monograph [41, Ch. 11] he wrote: “...I declare<sup>2</sup>, that turbulent solutions of fundamental equations include peculiarities or “almost peculiarities” of a completely different kind. These peculiarities are local scale non-invariant fractal sets and “almost peculiarities” are their approximations.” Mandelbrot formulated two specific assumptions: first, peculiarities of solutions of Euler equations were fractal sets; second, peculiarities of solutions of the Navier – Stokes equations could only be fractals.

In conclusion, we point out that the ideas of a fractal approach to turbulence have been expressed earlier. In the monograph by Frick P.G. “Turbulence: Approaches and Models” there is a section “Fractals and Turbulence”, and we are going to finish the review with a quote from it [42, P. 139]: “Kolmogorov model of homogeneous turbulence implies uniform filling of space with vortices of every scale... Different picture corresponds to turbulence with intermittency, in this case, some of the vortices do not receive energy from upper level vortices. At the next level, the energy of the remaining (active) vortices is again transferred only to a part of the vortices, and so on. As a result, a multiscale system of active and passive regions is formed in space. This system by structure is a fractal set. The idea of using fractals to describe the field structure was first expressed in the work of Novikov and Stuart in 1964 [43]. The simplest dynamical model of the inertial interval leading to fractals was proposed in [44]”.

### References

1. *Gladun A. D.* *Electronnaya tehnika*. 1966. Issue 8. P. 39-53 (in Russian).
2. *Miller M.* *Journal of Applied Physics*. 1961. Vol. 32, Issue 9. P. 1791-1793.

---

<sup>2</sup>Mandelbrot cited his own work «Mandelbrot B.B. Geometrie fractale de la turbulence. Dimension de Hausdorff, dispersion et nature des singularites dumouvement des fluides // Comptes Rendus (Paris). 1976. 282A. P. 119–120».

3. *Murie Zh.* Teoriya slabogo signala. In book *Electronnyye Sverchvysokochastotnyye Pribory so Skreschennymi Polyami*. M.: Izd-vo Inostrannoy literatury, 1961. Vol I, Parts V,XII (in Russian).
4. *Kyhl R. L. and Webster H. R.* IRE Transactions on Electron Devices. 1956. ED-3. P. 172-183.
5. *Levy R. H.* The Physics of Fields. 1965. Vol. 8, Issue 7. P. 1288-1295.
6. *Levy R. H. and Hockney R. W.* The Physics of Fields. 1968. Vol. 8. P. 766-771.
7. *Leyman V. G.* *Electronnaya Tekhnika*. 1968. Issue 8. P. 26-34 (in Russian).
8. *Gladun A. D., Leyman V. G.* *Zhurnal Tekhnicheskoy Fiziki*. 1970. Vol. 15, Issue 12. P. 2513-2517 (in Russian).
9. *Karbushev N. I., Udovichenko S. Yu.* *Zhurnal Tekhnicheskoy Fiziki*. 1983. Vol. 53, Issue 9. P. 1706-1709 (in Russian).
10. *Leiman V. G., Nikulin M. G., Rozanov N. E.* *Zhurnal Tekhnicheskoy Fiziki*. 1989. Vol. 59, Issue 4. P. 111-117 (in Russian).
11. *Kuznetsov S. P.* *Zhurnal Tekhnicheskoy Fiziki*. 1977. Vol. 47, Issue 12. P. 2483-2486 (in Russian).
12. *Kravchenya P. D.* Neustoichivosti v relyativistskih potokah v skreschennykh polayh. Dissertatsiya po special'nosti 01.04.04. Volgograd: Volgograd State University, 2014. 116 p. (in Russian).
13. *Shevchik V. N., Trubetskov D. I.* *Analiticheskie Metody Rascheta v Elektronike SVCH*. M.: Sov. Radio, 1970. 584 p. (in Russian).
14. *Pierce J. R.* IRE Transactions on Electron Devices. 1956. ED-4. P. 183-190.
15. *Krammer W.* Journal of Applied Physics. 1967. Vol. 37, Issue 5. P. 602-611.
16. *Leiman V. G.* *Electronnaya Tekhnika*. 1967. Seriya 1, Issue 8. P. 15-26 (in Russian).
17. *Singatullin R. M.* Chislennoe issledovanie dinamiki vkhrevykh struktur v sploshnykh sredah, vkluchaya plazmu. Dissertatsiya po special'nosti 25.00.29 and 01.04.03. Kazan: Kazan State University of Energetics. 116 p. (in Russian).
18. *Rabinovich M. I., Suschik M. M.* Kogerentnyye Struktury v Turbulentnykh Techeniyah. Nelineynye Volny. Samoorganizatsiya. M.: Nauka, 1983. P. 53-85 (in Russian).
19. *Kolesnichenko A. V.* Sinergeticheskii Podhod k Opisaniyu Stacionarno-Neravnovesnoi Turbulentnosti Astro-Geofizicheskikh Sistem. Preprint IMP named after Keldysh. M.: RAS, 2003. 37 p. (in Russian).
20. *Aburdzhaniya G. D.* Samoorganizatsia Nelineynykh Volnovykh Struktur i Vihrevoy Turbulentnosti v Dispergiruyuschih Sredah. M.: KomKniga, 2006. 328 p. (in Russian).
21. *Kervamishvili N. A.* *Zhurnal Tekhnicheskoy Fiziki*. 1990. Vol. 60, Issue 2. P. 78-84 (in Russian).
22. *Driscoll C. F., Fine K. S.* The Physics of Fields B. 1965. Vol. 2, Issue 6. P. 1359-1366.
23. *Golub Y. A., Nikulin M. G., Rozanov N. E.* *Zhurnal Tekhnicheskoy Fiziki*. 1990. Vol. 60, Issue 9. P. 78-82 (in Russian).
24. *Gordeev A. V.* Plasma Physics Reports. 2008. Vol. 34, Issue 6. P. 515-518.
25. *Benderskii B. Ya.* Aerogidrodinamika. Kurs Lekcii s Kratkimi Biografiyami i Interesnymi Sluchayami is Zhizni Uchenykh. M.-Izhevsk: NIC «Regulayrnaya i Haoticheskaya dinamika». 2012. 500 p. (in Russian).
26. *Kalinin Yu. A., Starodubov A. V.* Technical Physics. 2010. Vol. 55, Issue 12. P. 1788-1792.
27. *Kalinin Yu. A., Starodubov A. V., Mushtakov A. V.* Technical Physics. 2011. Vol. 56, Issue 6. P. 838-842.
28. *Kalinin Yu. A., Volkova L. N.* Technical Physics Letters. 2010. Vol. 36, Issue 7. P. 668-671.
29. *Kalinin Yu. A., Starodubov A. V., Volkova L. N.* Technical Physics Letters. 2010. Vol. 36, Iss. 10. P. 899-901.

30. *Kalinin Yu. A., Starodubov A. V.* Technical Physics Letters. 2011. Vol. 37, Issue 1. P. 91-93.
31. *Mchedlova E. S., Trubetskov D. I.* Zhurnal Tekhnicheskoi Fiziki. 1994. Vol. 64, Issue 10. P. 158-167 (in Russian).
32. *Kalinin Yu. A., Kildyakova O. A., Starodubov A. V., Trubetskov D. I.* Doklady Physics. 2016. Vol. 61, Issue 3. P. 112-115.
33. *Kaganov V. I.* Technical Physics Letters. 2006. Vol. 32, Issue 3. P. 252-254.
34. *Zhdanov S. K., Trubnikov B. A.* Quazigazovye Neustoychivye Sredy. M.: Nauka, 2001. 176 p. (in Russian).
35. *Trubnikov B. A.* Priroda. 2007. Issue 4. P. 68-73 (in Russian).
36. *Bulanov S. V., Sasorov P. V.* Zhurnal Eksperimentalnoi i Teoreticheskoi Fiziki. 1984. Vol. 86, Issue 2. P. 479-482 (in Russian).
37. *Kalinin Yu. A., Starodubov A. V., Fokin A. S.* Physics of Wave Phenomena. 2016. Vol. 24, Issue 3. P. 1-4.
38. *Kalinin Yu. A., Esin A. D.* Methods and Means of Physical Experiment in Vacuum Microwave Electronics. Saratov: Izd-vo Saratovsk. Gos. Univ., 1991 (in Russian).
39. *Kurkin S. A., Hramov A. E.* Bulletin Russian Academy of Sciences. Physics. 2011. Vol. 75(12). P. 1609.
40. *Stewart Ian.* The Great Mathematical Problems: Marvels and Mysteries of Mathematics. Profile Books Ltd, 2013. 340 p.
41. *Mandelbrot B. B.* Fraktal'naya Geometriya Prirody. Mosk-Izhevsk: Institut Kompyuternych Tekhnologii. 2002. 656 p. (in Russian).
42. *Frik P. G.* Turbulentnost': Podhody i Modeli. Mosk-Izhevsk: Institut Kompyuternych Tekhnologii. 2003. 292 p. (in Russian).
43. *Novikov E. L., Stuart R. V.* Izv. Akad. Nauk USSR. Seriya Geophysicheskaya. 1964. Issue 3. P. 408-413 (in Russian).
44. *Frisch U., Sulem P.-L., Nelkin M. J.* Fluid Mechanics. 1978. Vol. 87. P. 719-736.